Geophys. J. Int. (1996) **127**, 693–702

Estimation of period and Q of the Chandler wobble

M. Furuya[1] and B. F. Chao[2]

[1]*Department of Earth and Planetary Physics, University of Tokyo, Tokyo 113, Japan*

[2]*Laboratory for Terrestrial Physics, NASA Goddard Space Flight Center, Greenbelt, MD 20771, USA*

Accepted 1996 July 31. Received 1996 July 25; in original form 1995 December 25

SUMMARY

The period P and Q-value of the Chandler wobble are two fundamental functionals of the Earth's internal physical properties and global geodynamics. We revisit the problem of the estimation of P and Q, using 10.8 yr of modern polar motion as well as contemporary atmospheric angular momentum (AAM) data. We make full use of the knowledge that AAM is a major broad-band excitation source for the polar motion. We devise two optimization criteria under the assumption that, after removal of coherent seasonal and long-period signals, the non-AAM excitation is uncorrelated with the AAM. The procedures lead to optimal estimates for P and Q. Our best estimates, judging from comprehensive sets of Monte Carlo simulations, are $P = 433.7 \pm 1.8$ (1σ) days, $Q = 49$ with a 1σ range of (35, 100). In the process we also obtain (as a by-product) an estimate of roughly 0.8 for a 'mixing ratio' of the inverted-barometer (IB) effect in the AAM pressure term, indicating that the ocean behaves nearly as IB in polar motion excitation on temporal scales from months to years

Key words: atmospheric angular momentum, Chandler wobble, period, polar motion, Q-factor.

1 INTRODUCTION

The free Eulerian motion in the Earth's rotation, known as the Chandler wobble, was discovered in astrometric data by S. Chandler over 100 years ago. It has a period P of about 14 months as viewed from the terrestrial reference frame, and a finite quality factor Q due to inevitable energy dissipation. Chandler P and Q are two of the fundamental functionals for global geodynamics. Observations of their values are useful constraints in the inference of physical properties of the Earth's interior (e.g. Smith & Dahlen 1981; Okubo 1982; Zschau 1986): P depends sensitively on the mantle elasticity and anelasticity structure, the extent to which the fluid core is decoupled from the mantle, and how close the pole tide is to equilibrium, whereas Q contains information about the budget and processes of kinetic energy dissipation by the oceans, mantle anelasticity, and core–mantle coupling.

The International Latitude Service (ILS) began routine monitoring of the Earth's polar motion around 1900. Estimates of Chandler P and Q were made, once reasonably accurate data had been accumulated. Observationally, the Chandler wobble is a major component in the polar motion, along with the annual wobble and a polar drift. It has continued to exist since its discovery, and has exhibited a complex behaviour. Its amplitude varied slowly with an apparent 40 year modulation from a few tens to a few hundreds of milliarcseconds (mas). The spectrum exhibited multiple-component fine structure and a phase reversal around 1930. As its exact nature and excitation sources remain far from fully understood, this complex behaviour has posed great challenges to attempts to estimate Chandler P and Q.

Table 1 includes past estimates of P and Q using ILS data, by Jeffreys (1940, 1968), Ooe (1978), Wilson & Haubrich (1976), and Wilson & Vicente (1980, 1990). Two approaches were taken. The approach devised by Jeffreys (and later followed by Wilson & Haubrich 1976 and Wilson & Vicente 1990) seeks minimum variance for the excitation in a maximum-likelihood scheme. The approach used by Ooe (1978) and Wilson & Vicente (1980) adopts autoregressive–moving-average modelling for the observed polar motion. Both approaches assume Gaussian random excitations. This assumption, however, is hardly realistic. Physically, under the conservation of angular momentum, the excitation of Chandler wobble requires geophysical processes that involve mass movement in or on the Earth (e.g. Munk & MacDonald 1960). All geophysical processes are characterized by certain statistical properties. There is no *a priori* reason to expect randomness or 'Gaussian-ness'; the 'systematic' behaviour in the ILS observations described above attests to that fact.

To identify the Chandler excitation sources has remained an outstanding geophysical problem for decades. Only recently has the search been partially successful, as the variation of the atmospheric angular momentum (AAM) was found to be responsible for a major portion of the polar motion excitation,

Table 1. Summary of past and present estimates for the free Chandler wobble period and quality factor Q and 1σ uncertainty.

Study	Period (days)	Q (range)	Data (length in yr)
Jeffreys (1940)	446.7 ± 6.8	46 (37, 60)	ILS (42)
Jeffreys (1968)	433.2 ± 3.4	61 (37, 193)	ILS (68)
Wilson & Haubrich (1976)	434.0 ± 2.5	100 (50, 400)	ILS (70)
Ooe (1978)	434.8 ± 2.0	96 (50, 300)	ILS (76)
Wilson & Vicente (1980)	433.3 ± 3.6	175 (48, 1000)	ILS (78)
Wilson & Vicente (1990)	433.0 ± 1.1	179 (74, 789)	ILS+BIH (86)
Kuehne *et al.* (1996)	439.5 ± 1.2	---	Space93+AAM (9)
This Study	433.7 ± 1.8	49 (35, 100)	Space94+AAM (11)

especially on intraseasonal scales (Eubanks *et al.* 1988; Chao 1993; Kuehne, Wilson & Johnson 1993). Furuya, Hamano & Naito (1996) have found further evidence that suggests a strong influence of the wind term of AAM on the polar motion in and near the Chandler band.

These recent advances in the understanding of polar motion excitation have motivated us to revisit the estimation problem for Chandler P and Q. We shall not assume that the excitation source satisfies the neat statistical condition of being random and Gaussian. Rather, making full use of the knowledge that the AAM is a major excitation source for the polar motion, we devise two different estimators based on simple optimization criteria. The only assumption we will make is that the non-AAM excitation is uncorrelated with AAM (and we 'define' our AAM to conform to this condition, see below). Both estimators prove to be efficient and asymptotically unbiased; our adopted results (judged from a series of Monte Carlo experiments) are given in Table 1. It should be pointed out that one of our estimators is in principle equivalent to a recent, independent work by Kuehne *et al.* (1996; but see below), whose P estimate is also listed in Table 1.

2 FORMULATION

The polar motion is a 2-D quantity; expressing it in complex form greatly facilitates the numerical manipulation (Munk & MacDonald 1960). Thus, as customary, polar motion is expressed as $m=x+iy$ in radians, where x is the component of pole position along the Greenwich Meridian and y is that along 90°E. The polar motion excitation function as well as the AAM terms will all be similarly expressed in the same terrestrial coordinates. In the corresponding power spectrum, positive frequency means prograde motion while negative frequency means retrograde motion.

2.1 The problem

In order to utilize AAM, we must first 'define' our AAM. The AAM consists of the wind ('motion') term and the pressure ('mass') term; both are global integrals with respect to the entire atmosphere. The pressure term is customarily computed in two ways, depending on whether or not the oceanic inverted-barometer (IB) effect is assumed (e.g. Munk & MacDonald 1960). The IB effect is an idealized condition under which the sea level responds to overlying barometric loading in an isostatic manner. Air pressure variations anywhere over the ocean instantaneously spread out to the entire ocean area, greatly reducing the net effect compared to non-IB. Non-IB is the other idealized extreme, where the sea level, as if rigid, does not respond to barometric loads so that the load simply transmits directly to the ocean bottom. Without better knowledge, the total AAM is often taken as either 'wind + pressure' for the non-IB case, or 'wind + pressure IB' for the IB case. In exciting the polar motion, the pressure term dominates the wind term and hence the assumption of IB or non-IB makes a significant difference numerically (e.g. Chao & Au 1991). This is contrary to the situation with respect to the excitation of the length-of-day change (or the variation in the Earth's rotation rate), where the wind term dominates (*cf.* IERS 1995).

The reality presumably resides somewhere in between these two idealizations of IB and non-IB. To account for this in our present study, we build into the AAM a simple 'IB mixing ratio' γ such that the AAM is

$$\text{AAM} = (\text{wind term}) + \gamma\,(\text{pressure IB term}) + (1-\gamma)\,(\text{pressure term}). \quad (1)$$

With γ being an additional parameter with a value between 0 and 1 to be estimated in our optimization procedure, this simple linear model provides a crucial extra degree of freedom in determining what we consider the optimal AAM. In reality, γ is a variable depending on the temporal and spatial scales of the phenomenon in question. Here for simplicity we treat it as a constant, so that model (1) is approximately valid only in the frequency band of interest here. However, we allow γ to be complex-valued so that its (presumably small) imaginary part allows for any (east–west) phase differences among the terms in eq. (1).

It should be noted that, besides γ, certain 'transfer functions' in the form of constant coefficients are already built into the wind and pressure terms in eq. (1) (Munk & MacDonald 1960; Barnes *et al.* 1983). The transfer functions are functionals of the Earth's interior properties related to the Earth's Love numbers and the extent of the core–mantle coupling in the excitation process. Their departures from the theoretical values, here taken to be 1.591 and 1.098, respectively (Eubanks 1993), contain important geophysical information. Ideally, one would wish to be able to infer, or at least constrain, their true values from observations. By the same token, in eq. (1) we could have had two independent coefficients for the non-IB and IB pressure terms (and hence two degrees of freedom instead of

the restrained combination with coefficients γ and 1-γ). The problem of estimating these parameters is interesting in its own right, and awaits future studies. Here, however, as later Monte Carlo experiments will show, the values of P and Q are insensitive to the small parameter adjustments in the optimization. Therefore to estimate P and Q in a robust manner it suffices to hold fixed all parameters in AAM but one, namely γ, which 'absorbs' the overall indeterminacy.

We can now state the problem. We are given a polar motion time series $m(t)$. We know that $m(t)$ is the free Chandler wobble impulse response convolved with some excitation function, much of which is AAM. Schematically, the problem can be expressed in the numerical model:

$$D(P,Q)\ m(t)=\chi(t)=\mathrm{AAM}(\gamma,t)+\chi_{\mathrm{na}}(t), \qquad (2)$$

where AAM is given in eq. (1), which depends (linearly) on γ, χ is the excitation function, and χ_{na} is the non-AAM excitation plus random noise. D is the deconvolution filter that operates on m to yield χ. The discrete form for D can be readily derived from the polar motion equation of motion: $\chi(t)=(i/\omega)\,\partial_t m(t)+m(t)$ (e.g. Wilson & Haubrich 1976; also Wilson 1985), which depends (non-linearly) on P and Q through the complex frequency $\omega=2\pi(1+i/2Q)/P$. The task at hand is to find solutions for the three unknowns, P, Q and γ, subject to some criterion for optimization.

2.2 The optimization criteria

We employ two complementary optimization criteria (in the L_2 norm) to be described in this section. They are both based on the assumption that the non-AAM excitation χ_{na} is uncorrelated with the AAM excitation for the polar motion.

We first strive to remove non-random signals from χ so that χ_{na} can have a (nearly) flat power spectrum. AAM does not quite account for the observed annual wobble excitation (e.g. Chao & Au 1991), nor does it have much to do with the polar drift. Non-AAM geophysical excitation sources, such as variations of oceanic and hydrological angular momentum, post-glacial rebound, and core activities, often have their energy largely concentrated in seasonal and longer periods, leading to the annual wobble and other seasonal terms, and the polar 'drift' with periods comparable to or longer than the time span of our data series. Therefore, our strategy is to remove these signals at the outset from both χ and the AAM. We can (and will) also remove the long-period tidal signals from χ, even though they are relatively small to begin with (Chao 1994a). As another possible source, seismicity is presumably uncorrelated with AAM and is negligible during the period studied anyway (Chao, Gross & Han 1996).

Our numerical procedure in arriving at χ_{na} further ensures that χ_{na} and AAM will be uncorrelated. Through the optimization of the free parameter γ, our criteria essentially concentrate the signals in χ that are correlated with AAM terms in forming the optimal AAM. The remainder, i.e. χ_{na}, is therefore uncorrelated with AAM, or, strictly speaking, orthogonal to AAM in the L_2 norm. The χ_{na} obtained in this way has as little correlation with AAM as possible.

Criterion I

Criterion I seeks to minimize the non-AAM χ_{na} variance with respect to the variations in the three parameters P, Q and γ. The deconvolution is equivalent to a notch filter that removes the observed energy at P due to the Chandler resonance. Suppose, not knowing the true P and Q, that in the deconvolution we used P and Q that were somewhat in error. In that case the residual variance (after the removal of optimal AAM power), especially the spectral power in the Chandler frequency band, will not be completely removed. Under the assumption that the resultant errors are uncorrelated with the non-AAM excitation, this residual power will augment the true non-AAM excitation power, artificially elevating the variance. Therefore, the parameter values that minimize the residual variance constitute the optimal estimates under Criterion I.

In practice, instead of minimizing the total residual variance, we actually minimize only the residual spectral power in the Chandler frequency band. This narrow-band estimator has two advantages. It is obviously more sensitive because most error committed (by choosing incorrect P and Q in the deconvolution) is concentrated in the Chandler band. More important, however, is the following. As can be shown theoretically (Furuya 1996, in preparation), the existence of any residual excitation that is not accounted for (such as χ_{na} during the period studied in our present case) will bias the estimate for P and Q. The bias is approximately proportional to the ratio of the excitation variance to the polar motion variance. The latter ratio is lowest in the Chandler band (as a result of the Chandler resonance). Therefore a method that concentrates only on the Chandler band is extremely advantageous in reducing estimation biases. We should mention here that our procedure for removing AAM and other non-random signals, all above reasons aside, also helps in reducing the ratio mentioned above, and hence the bias.

Criterion II

Criterion II seeks to maximize the cross-correlation between the excitation function and AAM with respect to the variations in the three parameters P, Q and γ. As stated above, AAM has been found to have a broad-band cross-correlation with the observed excitation function. If, as above, the preselected P and Q used in deconvolution are somewhat in error, then the resultant excitation function χ will also be somewhat corrupted. Assuming that the non-AAM excitation χ_{na} is uncorrelated with AAM, this will in turn lead to a somewhat lower cross-correlation with AAM than the true correlation. Thus, maximizing this correlation with respect to P, Q and γ will serve as a criterion to yield estimates for the true P and Q. Note that the cross-correlation is complex-valued; it is the absolute value that we seek to maximize.

Possible bias in the estimates can result from dissimilarity in the overall spectra of χ and AAM, because the time-domain cross-correlation function makes use of the broad-band information with equal weight for all frequencies over the spectrum. This again accentuates the need for removing beforehand the harmonic and long-period signals. One must also be cautious when matching the two spectra (e.g. by filtering, see below), thus further reducing possible biases.

3 DATA AND NUMERICAL PROCEDURE

3.1 Data

The polar motion data we use are from the Space94 series (Gross 1996) obtained through a Kalman filter combination

of all modern space geodetic observations of the Earth's orientation that have been available since 1976. The data are given at nominal daily intervals; the effective Nyquist period is roughly 10 days because of the actual intervals between observations and the smoothing scheme employed in the Kalman filtering (Gross, personal communication, 1994).

We use the AAM data computed by the Japan Meteorological Agency (JMA) (Ozaki, Kuma & Naito 1994). This AAM series (the wind term, the pressure term, and the pressure IB term, for x, y and z components) are available from late 1983, and are given at 12 hr intervals until June 20, 1992 and at 6 hr intervals afterwards. The series are made into a daily series by taking averages for each day. A few minor data gaps have been linearly interpolated. To match the spectral content of the polar motion excitation, we low-pass the AAM series using a moderate fourth-order, zero-phase Butterworth filter at a cut-off period of 10 days. A parallel set of AAM series from the US National Meteorological Center (NMC) are also prepared in a similar way and used for comparison purposes.

The time span for the JMA series is 10.8 yr, from September 28, 1983, to June 30, 1994. This sets the limit for our present study, which is much shorter than the ILS data used by earlier workers (see Table 1). The shorter time span is a sacrifice we have to make in order to utilize AAM. It nevertheless avoids earlier polar motion data that are of considerably lower accuracy (IERS 1995). A rule-of-thumb minimum for the time span is 6 yr in order to separate the annual wobble from the Chandler wobble. A much longer time span is not a critical requirement in estimating P, but a time span at least as long as a reasonable fraction of Q cycles is highly desirable in yielding decent Q estimates, as will be illustrated below. Our series marginally meet the requirement for Q, as reflected in the range of uncertainties of the Q estimates.

3.2 Procedure

The first step is to deconvolve m to obtain the excitation function χ, as expressed on the left-hand side of eq. (2). This requires pre-selection of certain values for P and Q. For deconvolution D we adopt Filter (2) of Wilson (1985). This elementary filter has discrete phase distortions compared with more sophisticated filters. The actual differences, however, are insignificant for the frequency range of concern here, which is much lower than the Nyquist frequency.

We then remove from χ the harmonic signals of the annual wobble excitation and other seasonal terms, and the polar drift, as stipulated earlier. We achieve this by subtracting the least-squares fit of the following terms: sinusoidal terms with periods of $1/n$ yr with $n=1,2,\ldots,6$, and a third-degree polynomial of time representing the polar drift. In addition, two major tidal terms at fortnightly M_f periods (13.661 and 13.633 days) (see Chao 1994a; Gross, Hamdan & Boggs 1996) are removed simultaneously in a similar fashion.

At this point, we are ready to perform the optimization to yield optimal P, Q estimates. We perform two parallel procedures subject to the two optimization criteria.

(1) To use Criterion I we perform a non-linear, iterative search in the 3-D (P,Q,γ) space for the minimum of the residual spectral power R of the non-AAM excitation χ_{na}. The search is conducted by means of the simplex algorithm of Nelder & Mead (1965). R is evaluated by averaging the power spectrum over the Chandler band, which is here chosen to contain four elementary Fourier bins, from 0.67 to 0.94 cycle per year (cpy); we denote this scheme as Criterion Ia. The spectrum values themselves are computed using the multitaper technique of Thomson (1982), where seven orthogonal tapers with a time-bandwidth product of 4π are adopted. This procedure, by design, specifically ensures a minimum spectral leakage, which is highly desirable here. Two other schemes using much broader frequency bands in evaluating R are chosen for experimental comparisons: Criterion Ib uses 64 elementary bins from 0.49 to 6.11 cpy, while Criterion Ic uses 134 bins from -6.11 to 6.11 cpy, excluding four bins around the zero frequency simply to avoid any remnant polar drift signals.

(2) To use Criterion II, a non-linear, iterative search is conducted in a similar manner in the 3-D (P,Q,γ) space for the maximum of the absolute value of the cross-correlation function between the ensuing AAM and the excitation function χ, which invariably occurs as a prominent peak at zero time-shift (*cf.* Fig. 4 of Chao 1993).

3.3 Monte Carlo simulations

Before presenting our results, let us present a set of Monte Carlo numerical simulations of the above procedures. The main purpose is to assess the statistical properties of our estimators such as sensitivity, bias, and uncertainty in our estimates.

First we construct a synthetic AAM series using the JMA series with $\gamma_0=0.8+0.05i$. Suppose we then construct a polar motion series $m(t)$ by convolving this AAM with a free Chandler wobble with certain selected P_0 and Q_0, and a certain (reasonable) initial condition $m(0)$ whose exact value is immaterial to our experiment. Then both our estimation procedures applied to m and AAM should naturally recover the correct P_0, Q_0 and γ_0. This has been confirmed in a range of cases with the following exception: as the input Q_0 exceeds a few hundred, the recovered Q begins to fluctuate from Q_0 in a random fashion; the fluctuation is relatively small, but becomes progressively more severe as Q_0 becomes greater. We attribute this to the truncation errors.

Now suppose that the AAM is not the only excitation source, and that the non-AAM excitation is random and hence uncorrelated with AAM (as we have assumed all along). Numerically this is equivalent to perturbing the AAM with some random 'noise'. The resultant m will, of course, be perturbed accordingly. Our estimation procedures will then yield P and Q estimates that are somewhat corrupted from the true P_0 and Q_0. Varying the noise in a Monte Carlo iteration will then result in the statistics of our estimates.

The deciding factor in this Monte Carlo experiment is the level of the 'noise' to be added to the AAM, which we choose as follows. The maximum correlation coefficient between AAM and χ reaches as much as 0.66 through the proper choice of γ (see below). We performed a separate simple Monte Carlo simulation that finds the relationship between the correlation coefficient and the corrupting noise level. We found that, for the given number of points, a random series correlates at the 0.66 level with itself plus 110 per cent random noise. Therefore we adopt the latter as the noise level in our experiments: the noise added to the AAM has a standard deviation 1.1 times that of the AAM itself.

200 Monte Carlo simulations were performed using 'realistic' input judged from our results later: $P_0 = 434$ days and $Q_0 = 50$, leading to estimation statistics for the complex frequency ω and complex IB mixing ratio γ. Note that the real and imaginary parts of ω, proportional to $1/P$ and $1/PQ$, respectively, are the 'natural' variables that are characterized best by normal distributions; the corresponding statistics for the reciprocals P and Q are obtained from them. Fig. 1 shows the histograms of the 200 estimates for P, Q, real(γ), and imaginary (γ) by means of the Criterion Ia estimator. Figs 2 and 3 show the corresponding histograms for the Criteria Ib and Ic estimators, respectively. Fig. 4 shows the histograms for the Criterion II estimator.

Examining Figs 1(a)–4(a) for the P estimates, we find that the Criterion Ia result is the most accurate, as expected. Its distribution is tightly centred around the input P_0 of 434 days: the ensemble average is 434.04 days, with an ensemble standard deviation (1σ) of 1.8 days. The corresponding distributions of Figs 2(a) and 3(a) are 433.03 ± 2.1 days and 432.18 ± 3.1 days. The increasingly more significant skewness and biases with the broader band in which R is minimized confirm the aforementioned biasing effect due to excitations that are not accounted for (Section 2.2). The distribution of the Criterion II results is moderately biased, but has a much wider 1σ range: 435.02 ± 5.1 days.

Figs 1(b)–4(b) show the corresponding simulation results for Q. For clarity, only those smaller than 200 are plotted. In all cases the Q estimates are positive, but (particularly in 4b) there are instances where Q exceeds 200. Again Criterion Ia gives the most satisfactory estimates centred around the true $Q_0 = 50$: the ensemble average is 49, and the ensemble 1σ range is (36, 77). The broader-band estimates by Criteria Ib and Ic are somewhat biased: 56 (38, 101) and 52 (38, 84), respectively. Criterion II yields a distribution that is biased toward low Q values and is poorly constrained: 28 (14, 358).

Our estimators have a small bias for γ since it is a linear parameter, as shown in Figs 1(c)–4(c) for the real part and Figs 1(d)–4(d) for the imaginary part. The situation with the uncertainty is the opposite to that of P and Q: Criterion II gives the smallest σ, followed by the Ic, Ib, and finally Ia criteria. This is not surprising considering the broad-band nature of γ. In any event, the present paper is mainly concerned with P and Q estimates, which are insensitive to limited variations in γ judging from Figs 1–4.

We have performed two additional sets of Monte Carlo experiments. One is to assess possible bias in the Q estimation in cases where the input Q_0 is much greater than 50 (the above 'noise-free' simulations have demonstrated possible instability, but no indication of bias, as Q becomes very large.) This situation is of concern because then the total time span becomes much shorter than Q_0 cycles with a relatively small amount of decay during that time. In fact, the experiments performed by Kuehne *et al.* (1996) found a systematic bias towards lower Q estimates. Thus we repeated the Criterion Ia estimation for eight Q_0 values from 30 to 2000. The results show that one indeed sees a systematically lower Q estimate as Q_0 becomes larger, due presumably to the biasing effect mentioned in Section 2.2. This biasing trend is not as severe as that in Kuehne *et al.* (1996), and only affects Q_0 greater than ~ 300 (for which the corresponding estimates saturate at around 400), which is outside our present region of concern.

The other set of Monte Carlo experiments is to assess the importance of removing AAM from the excitation function before evaluating R in Criterion I. In one simulation, rather than removing the complete AAM, we only remove 0.5 AAM. The resultant estimates are considerably degraded. For example, in the Criterion Ia case the ensemble-averaged Q becomes 433.4 days with σ more than twice the previous value, while the ensemble-averaged Q becomes 73 and is poorly constrained. The Criterion Ib and Ic estimates are even poorer.

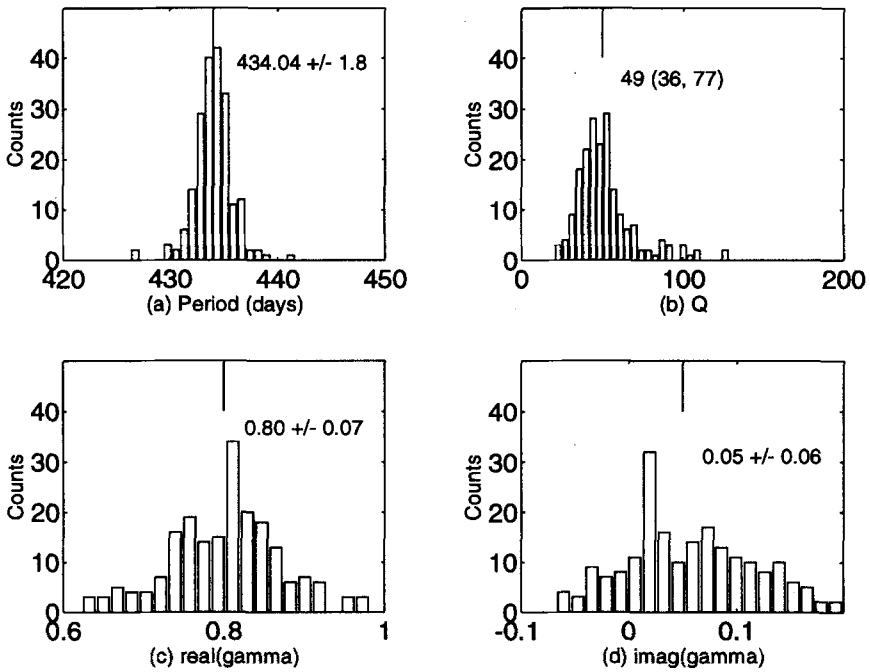

Figure 1. Histograms of 200 Monte Carlo simulation runs for the Criterion Ia estimator, for (a) P; (b) Q; (c) real part of γ; and (d) imaginary part of γ. In each figure, the ensemble average and standard deviation are given alongside the 'true' value indicated by the short vertical line.

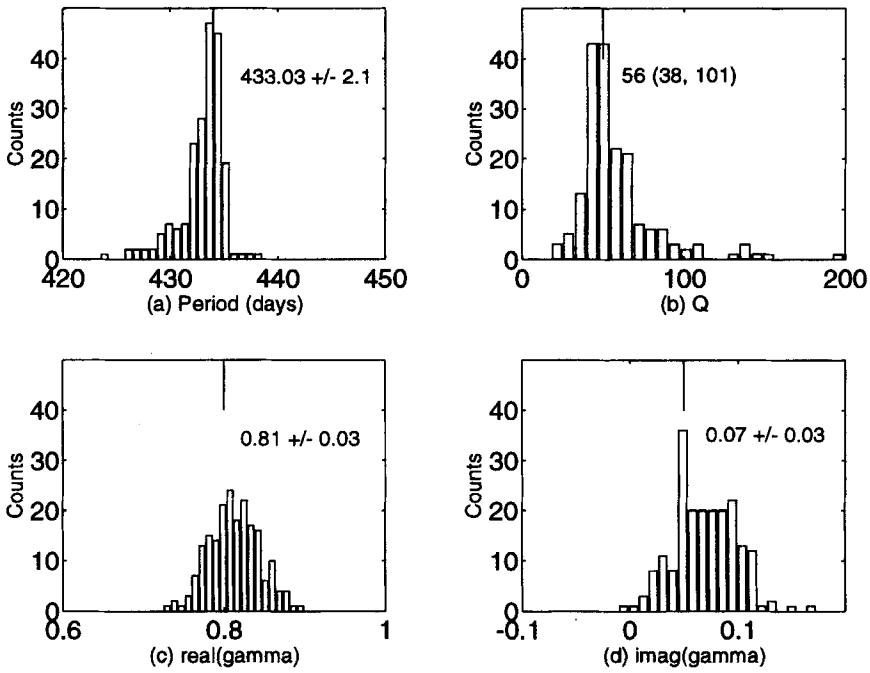

Figure 2. As Fig. 1, but for the Criterion Ib estimator.

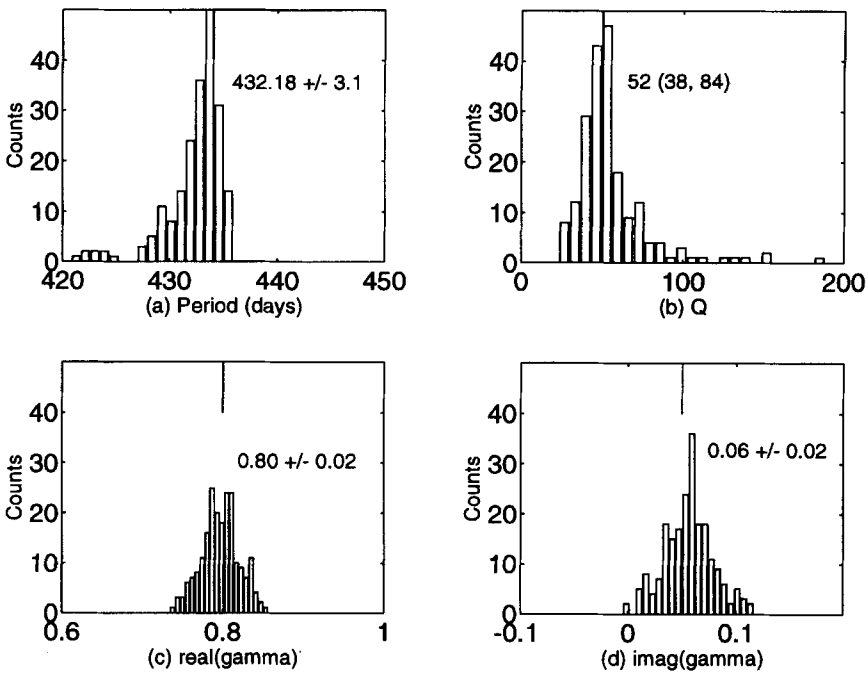

Figure 3. As Fig. 1, but for the Criterion Ic estimator.

When the amount of AAM removed is further reduced (to 0.25 AAM or 0), the degradation becomes increasingly severe, with Q estimates ranging into negative values, although the Criterion Ia estimator stays relatively robust for P.

4 RESULTS AND DISCUSSION

We apply our procedures to the Space94 polar motion series in conjunction with the JMA AAM data. Table 2 lists the results, which exhibit statistics very similar to our Monte Carlo simulations. Notably, the P estimates agree between the Criterion Ia and the Criterion II estimators. The broader-band Criterion Ib and Ic estimators are increasingly biased towards shorter periods. Criterion II yields considerably lower Q than Criterion I, and the AAM–χ correlation is found to be 0.66. The standard deviations in Table 2 are the nominal values adopted from our Monte Carlo simulations. As discussed above, we consider the P and Q estimates from Criterion Ia

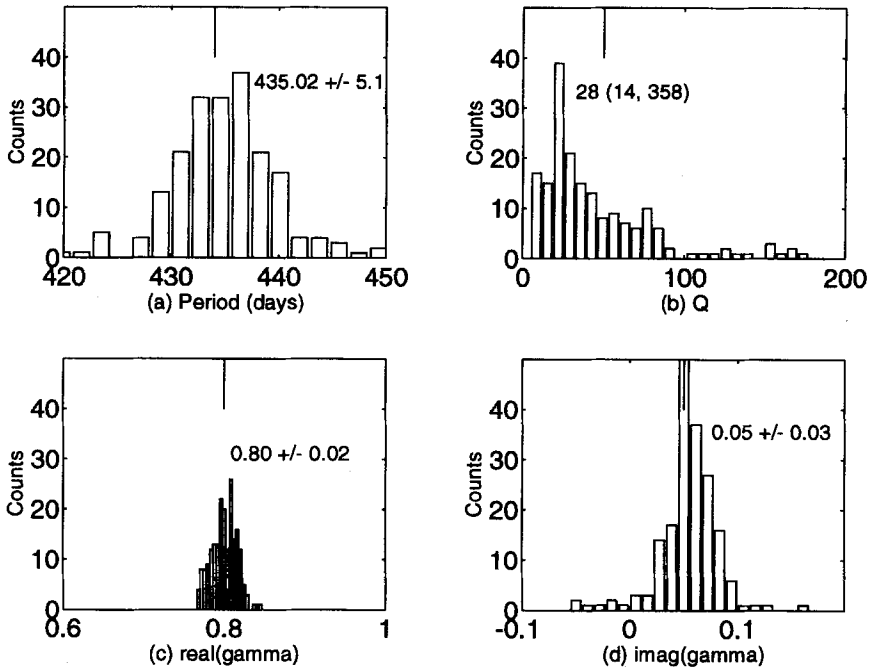

Figure 4. As Fig. 1, but for the Criterion II estimator.

Table 2. P, Q, and γ estimates with the nominal 1σ standard deviation from four different estimators employed in this study. The first set (with Q range properly scaled and corrected) is duplicated in Table 1.

Estimator	Period (days)	Q (range)	γ
Criterion Ia (4-bin)	433.7 ± 1.8	49 (36, 77)	$0.84 + 0.073i$
Criterion Ib (64-bin)	431.0 ± 2.1	42 (31, 64)	$0.93 + 0.16i$
Criterion Ic (134-bin)	430.8 ± 3.1	41 (31, 59)	$0.86 + 0.14i$
Criterion II	434.3 ± 5.1	27 (14, 239)	$0.74 + 0.047i$

to be the most accurate. The corresponding values, with the 1σ range of Q slightly broadened by scaling in accordance with the bias effect mentioned above, are duplicated in Table 1.

At this point, with the optimal determination of P, Q, and γ, we can present some of our key results in terms of the power spectrum, computed here using the multitaper technique (Thomson 1982). The spectrum of the observed excitation function $\chi(t)$ is displayed as the thin curve in Fig. 5(a) (the mean value of χ was removed beforehand). The frequency range is from -36 to 36 cpy, beyond which the power drops rapidly owing to the filtering process described above. Prominent signals of the polar drift, the annual and other seasonal terms, and the M_f tidal terms superimpose on a generally red spectral background. The thick curve in Fig. 5(a) shows the power spectrum of the non-AAM excitation $\chi_{na}(t)$, which as stipulated is the result of removing all the coherent signals and the optimal AAM (eq. 1). The overall redness of the spectrum is reduced, leaving a fairly flat spectrum. Fig. 5(b) shows the coherence (magnitude-squared) spectrum between the optimal AAM and $\chi(t)$ (again after removal of the coherent signals). One sees high broad-band coherence values relative to the confidence threshold of 0.54 for 99 per cent or 0.40 for 95 per cent, based on seven degrees of freedom (Chao & Eanes 1995).

Fig. 6 displays the shaded contour map of the Chandler residual power R as a function of P and Q, or the 2-D 'cross-section' of R in the (P,Q,γ) space, at the optimal value of $\gamma = 0.84 + 0.073i$, in which the minimization of R is carried out according to Criterion Ia. The minimum R occurs at the point marked by $\times$, corresponding to our optimal P and Q estimates given in Table 1. The first contour line corresponds approximately to 1σ. The simple, symmetric contour pattern reflects the robustness of the estimator.

For test purposes, the procedure is repeated by replacing the AAM data from JMA with those from NMC. The results become appreciably less satisfactory: now the minimum residual spectral power R (for Criterion I) is consistently higher than for JMA in all three bandwidths (Ia, Ib and Ic), and the maximum correlation between AAM and χ (for Criterion II) becomes significantly lower (0.59). The P estimates are consistently longer than the corresponding JMA values by 1–3 days, while the Q estimates have large variability and are much higher than their JMA counterparts, generally by an order of magnitude. The γ estimates are similar but have a somewhat larger range than those from JMA. The high Q estimates imply that the NMC AAM probably under-represents the true AAM power, especially in the Chandler band. In fact, the NMC analysis has been found to significantly underestimate the axial

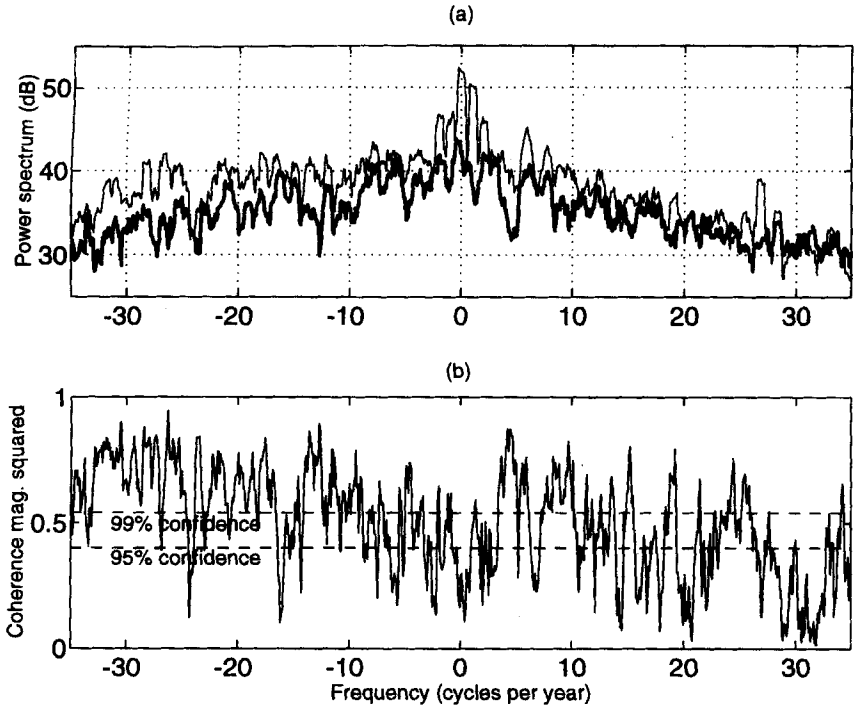

Figure 5. (a) The thin curve is the (multitapered) power spectrum of the observed polar motion excitation function (mean value removed). The thick curve is that of the non-AAM excitation function after all coherent signals and the optimal AAM are removed. (b) The coherence magnitude-squared spectrum between the observed and AAM-induced excitation functions, after all coherent signals are removed. The two horizontal lines indicate the confidence level of 99 per cent (0.54) and 95 per cent (0.40).

AAM variability (which affects the length-of-day) (Hide *et al.* 1996). Note that the results using the NMC AAM are reminiscent of the last set of Monte Carlo experiments, where deliberately lower levels of AAM were removed. We therefore consider these results to be less accurate and dismiss them here. Nevertheless, this experiment provides a sobering awareness of the adverse effects of inevitable errors in the AAM data in the present application.

From Table 1 we see that our best P estimate is not appreciably different from most previous estimates, considering the quoted uncertainties. Despite this numerical agreement, our Monte Carlo experiments illustrate the key improvement obtained by utilizing knowledge about AAM over past estimators that rely on the ILS series only. We maintain that, without applying knowledge about AAM, these past estimators can yield fairly accurate P estimates only because of the statistical advantage provided by the long time span of the data. Kuehne *et al.* (1996) used AAM as the primary excitation in a least-squares estimation, which can be shown to be equivalent to our Criterion II (in L_2 norm), but obtained a quite different P estimate (see Table 1). Besides relatively minor differences, the key difference between the work of Kuehne *et al.* (1996) and our present study is the fact that Kuehne *et al.* do not remove the seasonal signals in their procedure, making their estimation prone to skewing due to the presence of these signals, especially the dominant annual wobble which is close to the Chandler wobble in frequency.

The problem with Q estimation is more complicated. The variation of the wobble amplitude is the result of the combined effects of excitation (via convolution) and natural wobble decay (via modulation). Numerically these two effects are inseparable; hence a Q estimation is not possible unless one assumes certain statistical properties of the excitation, such as randomness with minimum variance.

Our Q estimates are considerably lower than most previous estimates based on ILS data [except the good agreement with the earliest estimates by Jeffreys (1940, 1968), which we believe is fortuitous]. This is not surprising and can be understood as follows. For time spans comparable to or longer than Q cycles, the excitation is an important factor that maintains the wobble at amplitudes higher than would be the case without the excitation. Therefore, failure to account for the excitation properly, for example by minimizing the variance of excitation which is far from random (see Section 1), would readily lead to a falsely high Q estimate. In fact, it is interesting to note that the past Q estimates based on ILS data indeed become larger almost monotonically as longer data series are used (see Table 1).

Finally, we note that the γ estimates range mostly around 0.7 to 0.9. This means that the overall behaviour of the ocean is close to IB, at roughly the 80 per cent level, in polar motion excitation on timescales of months to years. The imaginary part of γ is small, signifying small east–west phase differences between AAM and the observed excitation. These are consistent with findings with respect to the length-of-day variations (Chao 1994b) and the variations in the Earth's dynamic oblateness J_2 (Chao & Eanes 1995).

Our methodology provides effective estimators for Chandler P and Q. To improve our present estimates would require AAM data with higher accuracy and a much longer time span. Higher accuracy can presumably be achieved with the new re-analysis of global meterological data now underway at meterological centres, such as NMC (now NCEP) and the NASA Goddard Data Assimilation System, with improved

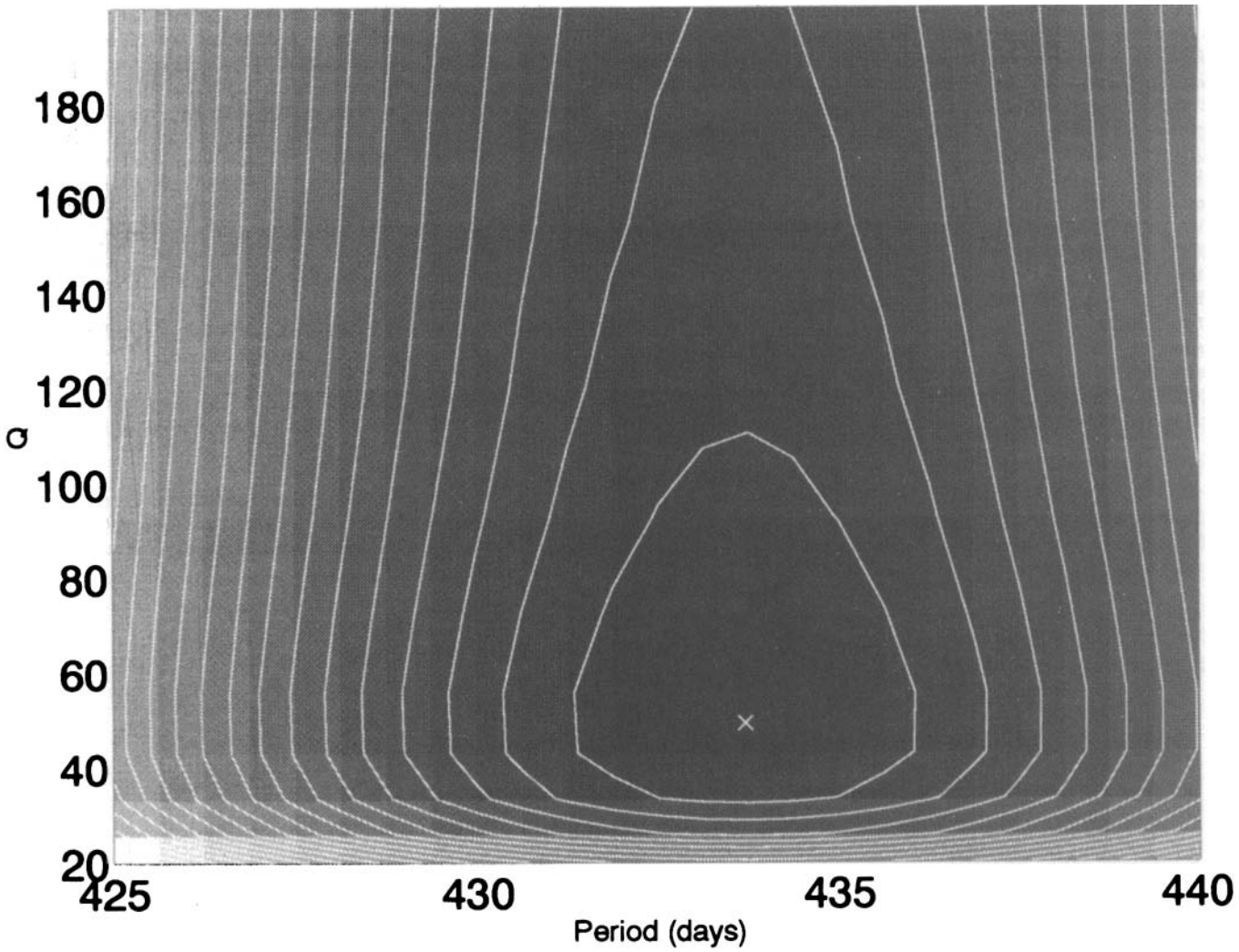

Figure 6. Shaded contour map of the residual non-AAM power R in the Chandler band for the Criterion Ia estimator, as a function of P and Q, holding γ fixed at the optimal value. The × marks the minimum R, corresponding to the optimal estimates for P and Q. The first contour corresponds to 1σ.

general circulation models and data assimilation algorithms. Longer time spans can be expected when these AAM data series are extended backwards in time and, of course, into the future.

ACKNOWLEDGMENTS

We thank R. Gross for providing the Space94 polar motion data, I. Naito for the JMA AAM data, and D. Salstein for the NMC AAM data. We also thank C. Wilson for discussions and suggestions. This work was conducted while one of us (MF) was on leave at the NASA Goddard Space Flight Center under the support of the NASA Geophysics Program and a Young Scientist Fellowship from the Japan Society for Promotion of Sciences through Professor Yozo Hamano.

REFERENCES

Barnes, R.T.H., Hide, R., White, A.A. & Wilson, C.A., 1983. Atmospheric angular momentum fluctuations, length-of-day changes and polar motion, *Proc. R. Soc. Lond.*, A, **387,** 31–73.

Chao, B.F., 1993. Excitation of Earth's polar motion by atmospheric angular momentum variations, 1980–1990, *Geophys. Res. Lett.*, **20,** 253–256.

Chao, B.F., 1994a. Zonal tidal signals in the Earth's polar motion, *EOS, Trans. Am. geophys. Un.* **75,** 158.

Chao, B.F., 1994b. Transfer function for length-of-day variations: Inference for Earth dynamics, *EOS, Trans. Am. geophys. Un.*, **75,** 111.

Chao, B.F. & Au, A.Y., 1991. Atmospheric excitation of the Earth's annual wobble: 1980–1988, *J. geophys. Res.*, **96,** 6577–6582.

Chao, B.F. & Eanes, R.J., 1995. Global gravitational change due to atmospheric mass redistribution as observed in Lageos' nodal residual, *Geophys. J. Int.*, **122,** 755–764.

Chao, B.F., Gross, R.S., & Han, Y.B., 1996. Seismic excitation of the polar motion, 1977–1993, *Pure appl. Geophys.*, **146,** 407–419.

Eubanks, T.M., 1993. Variations in the orientation of the Earth, in *Contributions of Space Geodesy to Geodynamics: Earth Dynamics,* pp. 1–54, eds Smith D.E. & Turcott, D.L., AGU, Washington, D.C.

Eubanks, T.M., Steppe, J.A., Dickey, J.O., Rosen, R.D. & Salstein, D.A., 1988. Causes of rapid motions of the Earth's pole, *Nature,* **334,** 115–119.

Furuya, M., Hamano, Y. & Naito, I., 1996. Quasi-periodic wind signal as a possible excitation of Chandler wobble, *J. geophys. Res.*, in press.

Gross, R.S., 1996. Combinations of Earth orientation measurements: SPACE94, COMB94, and POLE94, *J. geophys. Res.*, **101,** 8729–8740.

Gross, R.S., Hamdan, K.H. & Boggs, D.H., 1996. Evidence for excitation of polar motion by fortnightly ocean tides, *Geophys. Res. Lett.*, **23**, 1809–1812.

Hide, R., Dickey, J.O., Marcus, S.L., Rosen, R.D. & Salstein, D., 1996. Angular momentum fluctuations in global numerical general atmospheric circulation models during the AMIP period 1979–89, *J. geophys. Res.*, submitted.

IERS, 1995. Earth orientation, reference frames and atmospheric excitation functions submitted for the 1994 IERS Annual report, Int. Earth Rotation Service, *Tech. Note 19*, Paris.

Jeffreys, H., 1940. The variation of latitude, *Mon. Not. R. astr. Soc.*, **100**, 139–155.

Jeffreys, H., 1968. The variation of latitude, *Mon. Not. R. astr. Soc.*, **141**, 255–268.

Kuehne, J., Wilson, C.R. & Johnson, S., 1993. Atmospheric excitation of nonseasonal polar motion, *J. geophys. Res.*, **98**, 973–978.

Kuehne, J., Wilson, C.R. & Johnson, S., 1996. Estimates of the Chandler wobble frequency and *Q*, *J. geophys. Res.*, **101**, 13 573–13 579.

Munk, W.H. & MacDonald, G.J.F., 1960. *The Rotation of the Earth*, Cambridge Univ. Press, New York, NY.

Nelder, J.A. & Mead, R., 1965. A simplex method for function minimization, *Comput. J.*, **7**, 308–313.

Okubo, S., 1982. Theoretical and observed *Q* of the Chandler wobble—Love number approach, *Geophys. J. R. astr. Soc.*, **71**, 647–657.

Ooe, M., 1978. An optimal complex, AR.MA model for the Chandler wobble, *Geophys. J.R. astr. Soc.*, **53**, 445–457.

Ozaki, T., Kuma, K. & Naito, I., 1994. Effective atmospheric angular momentum functions computed from the Japan Meteorological Agency data, *IERS Tech. Note 16*, Observatoire de Paris.

Smith, M.L. & Dahlen, F.A., 1981. The period and Q of the Chandler wobble, *Geophys. J. R. astr. Soc.*, **64**, 223–281.

Thomson, D.J., 1982. Spectrum estimation and harmonic analysis, *Proc. IEEE*, **70**, 1055–1096.

Wilson, C.R., 1985. Discrete polar motion equations, *Geophys. J. R. astr. Soc.*, **80**, 551–554.

Wilson, C.R. & Haubrich, R.A., 1976. Meteorological excitation of the Earth's wobble, *Geophys. J.R. astr. Soc.*, **46**, 707–743.

Wilson, C.R. & Vicente, R.O., 1980. An analysis of the homogeneous ILS polar motion series, *Geophys. J. R. astr. Soc.*, **62**, 605–616.

Wilson, C.R. & Vicente, R.O., 1990. Maximum likelihood estimates of polar motion parameters, in *Geophys. Monogr.* **59**, pp. 151–155, AGU Washington, DC.

Zschau, J., 1986. Tidal friction in the solid Earth: Constraints from the Chandler wobble period, in *Space Geodesy and Geodynamics*, pp. 315–344, eds Anderson, A. & Cazenave, A., Academic Press, London.